Temporal flowability evolution of slag-based self-compacting concrete with recycled concrete aggregate

Víctor Revilla-Cuesta [a], Marta Skaf [b, *], Amaia Santamaría [c], Jorge J. Hernández-Bagaces [b], Vanesa Ortega-López [a]

[a] Department of Civil Engineering, University of Burgos, EPS. Calle Villadiego s/n. 09001, Burgos, Spain
[b] Department of Construction, University of Burgos, EPS. Calle Villadiego s/n. 09001 Burgos, Spain
[c] Department of Mechanical Engineering, University of the Basque Country, UPV/EHU, Escuela de Ingeniería de Bilbao, I (bloque B) - UPV/EHU, Plaza Ingeniero Torres Quevedo, 1, 48013 Bilbao, Spain

ABSTRACT

The addition of by-products, such as recycled concrete aggregate and ground granulated blast furnace slag, modify the in-fresh flowability of ordinary self-compacting concrete both initially and over time. A detailed study is presented in this paper of 18 mixtures (SF3 slump-flow class) containing 100% coarse recycled concrete aggregate, two types of cement (CEM I or CEM III/A, the latter with 45% ground granulated blast furnace slag), different contents of fine recycled concrete aggregate (0, 50, or 100%), and three different aggregate powders (ultra-fine limestone powder <0.063 mm, limestone fines 0/0.5 mm, and recycled concrete aggregate 0/0.5 mm). The temporal evolution of slump flow, viscosity, and passing ability, and the values of segregation resistance, air content, fresh and hardened density, and compressive strength were evaluated in all the mixtures. The addition of fine recycled concrete aggregate and CEM III/A improved initial slump flow and passing ability by 6%, due to their higher proportion of fines. Nevertheless, the temporal loss of flowability within 60 min was 5.8% lower when adding natural aggregate and CEM I. Viscosity and air content increased 26% on average following additions of fine recycled concrete aggregate, unlike with additions of ground granulated blast furnace slag. Flowability and strength increased with the addition of limestone fines 0/0.5 mm. According to multi-criteria analyses, the mixtures with CEM III/A, 50% fine recycled concrete aggregate, and limestone fines 0/0.5 mm showed an optimal balance between their flowability (SF2 slump-flow class 60 min after the mixing process), compressive strengths (around 60 MPa), and carbon footprints.

© 2021 The Authors. Published by Elsevier Ltd. This is an open access article under the CC BY-NC-ND license (http://creativecommons.org/licenses/by-nc-nd/4.0/).

1. Introduction

Concrete is the most extensively used structural material within the construction sector and its components form recurrent design features found in many buildings and civil works. Annual concrete consumption stands at around 890 Mt in Europe alone (ERMCO, 2019). However, this material also has some significant environmental impacts. The manufacture of 1 t (1000 kg) of cement clinker emits 0.9 t of CO_2 into the atmosphere (Maddalena et al., 2018) and Natural Aggregate (NA) extracted from quarries or gravel pits usually represents between 60 and 70% of concrete volume (ANEFA, 2019). One way of adding to the sustainability of concrete is to substitute traditional clinker for residues with pozzolanic properties and, more recently, for alkali-activated wastes (Elahi et al., 2020). Another alternative is to replace NA with different by-products (Gupta et al., 2020), such as slag (Roslan et al., 2020) and construction and demolition waste (Gonzalez-Corominas et al., 2017). The application of either strategy curtails waste generation in a consumer society where it is problematic (Khan et al., 2019), such as the 865 Mt of construction and demolition waste generated in Europe alone on an annual basis (Eurostat, 2019).

Following the initial research work of Ouchi et al. (2000), Self-Compacting Concrete (SCC) emerged between the end of the 20th century and the beginning of the 21st century. It is one of the most

sustainable types of concrete, due to its high flowability in the fresh state, in so far as no vibration is needed for its placement, which significantly reduces energy consumption (Huang et al., 2018). High flowability is ensured through the addition of a suitable admixture and an adequate balance between the coarse, fine, and powder fractions of the aggregate. The appropriate average proportions of these components are 30% by volume of coarse aggregate and a powder content of 500 kg/m^3 (EFNARC, 2002). Proper retention of flowability over time is a key aspect of this type of concrete, so that flowability is retained while in transportation from the manufacturing plant to the site for placement (EFNARC, 2002). It is therefore essential to adapt the mix design to the characteristics of each component, in order to produce an SCC of adequate flowability over a prolonged period of time (Santos et al., 2019a). Other problems should likewise be minimized, such as high air content, resulting mainly from the high admixture and water content that is typical of SCC (Huang et al., 2018).

Ground Granulated Blast Furnace Slag (GGBFS) is a type of slag resulting from fast cooling and subsequent grinding of blast furnace slag. Its grinding fineness is very high and its pozzolanic properties make it a good substitute for cement clinker (Parron-Rubio et al., 2018). CEM III, a standardized cement type, incorporates between 35 and 95% GGBFS in accordance with EN 197−1 (EN-Euronorm). This type of cement has traditionally been used for marine concrete structures submerged in seawater (Pacheco and Polder, 2016). More recently, it has been employed in the stabilization of both clayey (Du et al., 2020) and contaminated soils (Wu et al., 2018) and in the manufacture of road bases and sub-bases (Abdollahnejad et al., 2020). Its use in the production of SCC is not widespread (Reddy et al., 2020) and its effect on the temporal flowability of SCC is yet to be studied.

Recycled Concrete Aggregate (RCA) is a by-product from the demolition of aging concrete structures (Khan et al., 2019). However, the crushing of rejected concrete elements mainly from the precast concrete industry yields the highest quality RCA (Fiol et al., 2018). If the mix design of SCC is adjusted to the particular characteristics of this residue, mainly to its high water absorption levels (Sainz-Aja et al., 2019), then RCA is a valid alternative by-product for the manufacturing of SCC (Salesa et al., 2017). If coarse RCA is used, the higher its content, the worse the temporal retention of flowability. The use of the coarse fraction of this waste at room humidity without pre-soaking worsens its in-fresh performance due to a loss of flowability, as higher levels of mix-water are slowly absorbed into the RCA (González-Taboada et al., 2017a). Nevertheless, pre-soaking of coarse RCA yields a good temporal conservation of flowability (45 min after the end of the mixing process, the loss of slump flow was only around 9% for 100% coarse RCA), although it hinders any industrial usage (González-Taboada et al., 2017a). The use of only fine RCA in SCC also hinders the temporal retention of flowability: 45 min after the start of the mixing process, the slump flow decreased by 8% and 28% in the mixtures with 50% and 100% fine RCA respectively (Carro-López et al., 2015). In both studies, no mixing process to improve SCC flowability without pre-soaking RCA was considered, although the initial flowability of SCC with 100% coarse RCA can be maximized through adjustments to the water content and the use of two-stage mixing processes (Güneyisi et al., 2014). It may be mentioned that there are no studies to date on the joint use of both RCA fractions, their interaction, and their effects on SCC flowability.

The hardened properties of SCC are fundamental when defining the mix design (Revilla-Cuesta et al., 2020c), as SCC is very sensitive to the slightest variation in mix composition, such as water, cement, plasticizer content, or coarse-to-fine aggregate ratio (Fiol et al., 2018). A precise definition of the amount of coarse and fine RCA

added to the mix according to their specific characteristics is therefore essential to obtain high compressive strength with no loss of flowability (Santos et al., 2019a). While concrete with a high compressive strength of over 45 MPa was obtained with 100% coarse RCA, the addition of fine RCA had more adverse effects, even at low-level replacements of 30% (Silva et al., 2015). Nevertheless, the optimization of the mix design with 100% coarse RCA, 50% fine RCA, and standard amounts of cement yielded an SCC with a slump flow of between 650 and 750 mm (SF2 slump-flow class) and a compressive strength of over 45 MPa (Revilla-Cuesta et al., 2020a).

The objective of this study is to ascertain whether it is possible to produce a sustainable SCC with high flowability over time and an adequate compressive strength. To do so, an SF3 slump-flow class SCC was produced, using the two by-products described in detail in this introduction: coarse and fine RCA, and GGBFS. Furthermore, the effects of various aggregate powders used as sustainable alternatives to conventional ultra-fine limestone powder (i.e., limestone filler) were also analyzed. The few evaluative studies on the temporal fresh behavior of medium-flowability SCC have been limited to the effect of only one RCA fraction (coarse or fine) with no additions of sustainable binders (GGBFS) or aggregate powders to the mixtures (Carro-López et al., 2015; González-Taboada et al., 2017a). Accordingly, the novelties of this study are as follows:

- Firstly, the fresh behavior over time of SCC manufactured with both coarse and fine RCA was studied. The simultaneous use of both RCA fractions can alter the performance of SCC in comparison with the use of only one fraction.
- Secondly, the influence of GGBFS as binder and aggregate powders more sustainable than standard ultra-fine limestone powder (limestone fines 0/0.5 mm, and RCA 0/0.5 mm) on the temporal flowability of SCC was evaluated. Their interactions with RCA were also analyzed.
- Both previous aspects were applied for the first time to a highly SCC (SF3 slump-flow class), the flowability of which is very sensitive to changes in its composition (Revilla-Cuesta et al., 2020c). The addition of each by-product therefore notably alters its fresh behavior, so that the effect of each product on SCC flowability can be measured in detail.
- Finally, a statistical model was developed from the experimental results, to predict the loss of flowability of the SCC manufactured with RCA. In addition, the results of a multi-criteria analysis confirmed the suitability of the mixtures under development. Both approaches are also new in the literature.

In this study, 18 highly SCC mixes were produced to investigate the above aspects of their flowability. All of them contained 100% coarse RCA, while different percentages of fine RCA (0, 50, and 100%) were added in substitution of siliceous sand. CEM III/A, with 45% GGBFS, as per EN 197−1 (EN-Euronorm), was incorporated in half of the mixtures. The effects on SCC flowability of three different aggregate powders (ultra-fine limestone powder <0.063 mm, limestone fines 0/0.5 mm, and RCA 0/0.5 mm) were also evaluated. Lastly, a three-stage mixing process was designed to assess improvements to the temporal flowability of the SCC samples following maximization of RCA water absorption (Güneyisi et al., 2014).

2. Materials and methods

The raw materials, the composition of the SCC mixtures, and the experimental procedure that yielded the final results are all presented in this section.

2.1. Materials

The raw materials of the SCC mixes designed can be divided in three groups:

- Two different types of cement, CEM I 52.5 R and CEM III/A 42.5 N, were used. The latter had a GGBFS content of 45%. Two different admixtures provided self-compactability to the mixes.
- Three different aggregate powders were considered: ultra-fine limestone powder <0.063 mm, limestone fines 0/0.5 mm, and RCA 0/0.5 mm.
- 100% coarse aggregate was RCA in all mixes, while the fine aggregate was siliceous sand and/or fine RCA.

Full details of the characteristics of these materials can be found in the supplementary data.

2.2. Mix design

All the mixtures were designed to have a SF3 slump-flow class (slump flow between 750 and 850 mm), as defined in EFNARC (2002). The fresh behavior of all the mixes could therefore be compared between each other (same slump-flow class), and the fresh behavior of this type of SCC, usually very susceptible to changes in its composition (Santamaría et al., 2020b), could be analyzed. An optimal fit with the Fuller curve in relation to the percentage of particles smaller than 0.25 mm (see Fig. 1) was a pre-requisite to achieve this high slump flow. The initial proportions of the mix components, based on EC-2 (2010), were empirically adapted.

All the SCC mixtures shared some aspects of this composition. On the one hand, they all incorporated 100% coarse RCA. This content was defined on the basis of the high compressive strength of the SCC that was manufactured with this amount of waste together with 100% fine NA, as demonstrated in another study by the authors (Revilla-Cuesta et al., 2020a). On the other, the fine RCA 0/4 mm was simultaneously added in substitution of the siliceous sand 0/4 mm, a commonly used practice in the industrial manufacture of precast concrete (Fiol et al., 2018). According to the data collected in Fig. 1 regarding the F mixes as representative examples, the replacement of siliceous sand by fine RCA increased the content of particles smaller than 0.25 mm in the mix, unlike a substitution of equal sized particles (Santos et al., 2019b). This circumstance slightly improved the initial fresh behavior of the fine RCA mixes in some tests (slump-flow and L-box tests), as shown in later sections. Hence, the temporal results of these tests are discussed on the basis of the (relative) percentile variations of these properties. Each mix composition was adjusted in three different ways, so all the mixes had different designs. All substitutions were performed with the volume correction technique.

- Firstly, the water content was adjusted to compensate for the water absorption of the RCA. The effective water-to-cement ratio remained constant in all the mixtures produced with the same type of cement (0.50 for CEM I mixtures, and 0.40 for CEM III mixtures). Its calculation involved subtracting the water absorbed into the aggregate under room-moisture conditions throughout the 15-min mixing time from the total water content of the mix (Fig. 2).
- Secondly, the optimal content of each aggregate powder was determined according to its percentage particle content lower than 0.25 mm. All of them yielded a SF3 slump-flow class SCC.
- Finally, the use of CEM III/A hindered the uniform dragging of the aggregate particles in the slump-flow test, due to the higher grinding fineness of CEM III/A in comparison with CEM I (Dai

et al., 2019). A reduction in the coarse RCA content used in the mixtures allowed solving this problem.

A total of 18 mixes were designed with different combinations of cement, fine RCA percentages, and aggregate powder. These mixes were labelled C−N/T:

- C represents the type of cement used: I (CEM I), or III (CEM III/A).
- N is the percentage of fine RCA added to the mix: 0, 50, or 100.
- T indicates the nature of the aggregate powder in use: F (ultra-fine limestone powder), L (limestone fines 0/0.5 mm), or R (RCA 0/0.5 mm).

The composition of the mixes is shown in Table 1, Table 2, and Table 3. All the mixtures had a high content of by-products as substitutes for natural materials, with the aim of maximizing the sustainability of the mixtures. The maximum RCA content in mix I-100/R represented 62% of the total volume.

2.3. Experimental plan

As previously indicated, multi-stage mixing processes minimize the effects of RCA and its high water absorption levels on the fresh behavior of concrete (Güneyisi et al., 2014). For this reason, the components of the mix were added to the concrete mixer in three stages. In the first stage, the coarse and fine aggregate, the aggregate powder, and half of the water were added. In the second stage, the cement and the rest of the water were included. In the third stage, the admixtures were finally added. After each stage, the concrete was mixed for 3 min and then left to rest for 2 min. These times maximized the slump flow and were obtained after several attempts with mixing and resting times between 1 and 5 min. With this multi-stage mixing process, the aggregates absorbed water for 15 min before the tests in the fresh state were performed. Moreover, the hydration of the cement and the effect of the admixtures were also maximized, which also improved the flowability of the SCC (Huang et al., 2018).

After mixing, the tests in the fresh state were performed: slump-flow, V-funnel, 2-bar L-box, sieve-segregation, air-content, and fresh-density tests. The slump-flow test was carried out at four different points in time to analyze its temporal evolution, while the V-funnel and the 2-bar L-box tests were performed twice with an interval of 45 min. A strict experimental plan was defined (Fig. 2), so that each mix could be compared with the others: each test in the fresh state was performed at the same time in all the mixes.

Apart from correct flowability, density and a compressive strength of SCC must be suitable for its use (Santamaría et al., 2020a). Therefore, the two aforementioned properties were determined for all the mixtures in 10 × 10 × 10-cm cubic specimens at 28 days. The specimens were manufactured between 30 and 50 min after the end of the mixing process.

3. Results and discussion: fresh behavior

The fresh-state tests were performed to evaluate the filling ability, viscosity, passing ability, and segregation resistance of the SCC. The applicable regulations for the performance of each test and the SCC classifications according to EFNARC (2002) are shown in Table 4. Additionally, the fresh density and the air content were determined according to the specifications of EN 12350−6 and EN 12350−7 (EN-Euronorm), respectively. Specifications of the standardized test equipment are shown in Fig. 3.

3.1. Filling ability and viscosity: slump-flow test over time

The slump-flow test, according to EN 12350−8 (EN-Euronorm), is fundamental in an evaluation of the filling ability of SCC without
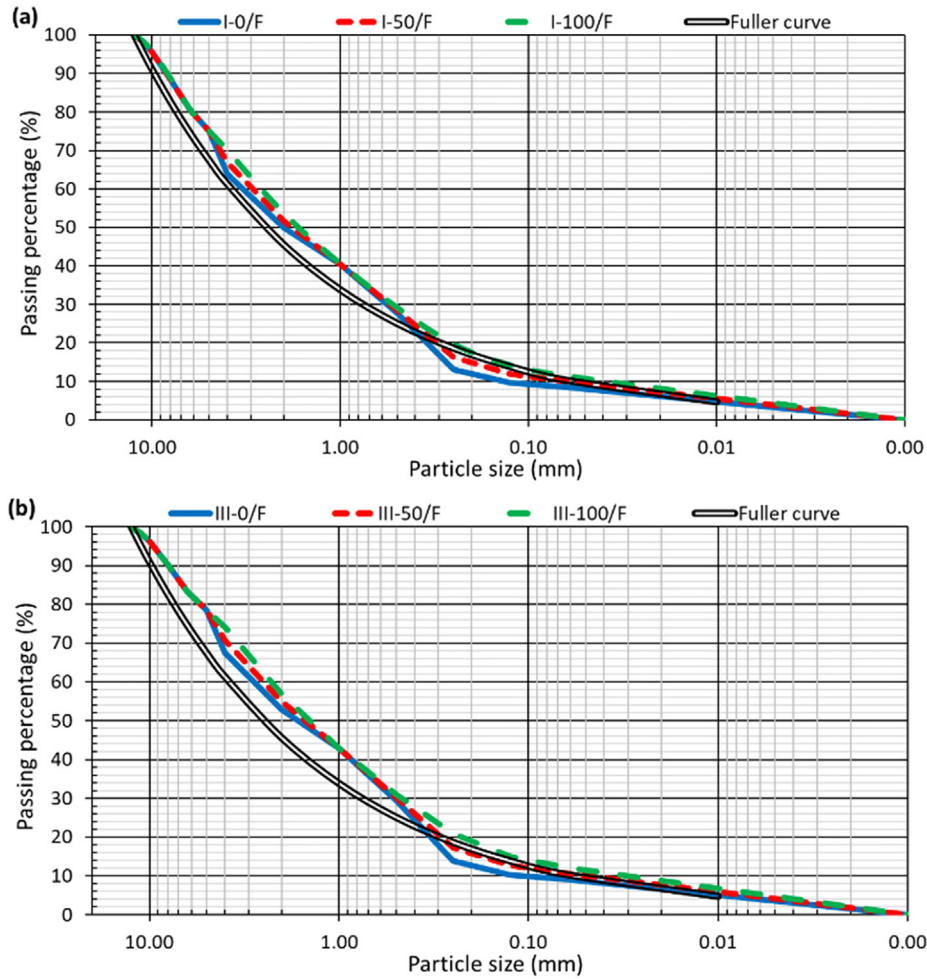
Fig. 1. Gradation of the mixes with ultra-fine limestone powder: (a) CEM I; (b) CEM III.
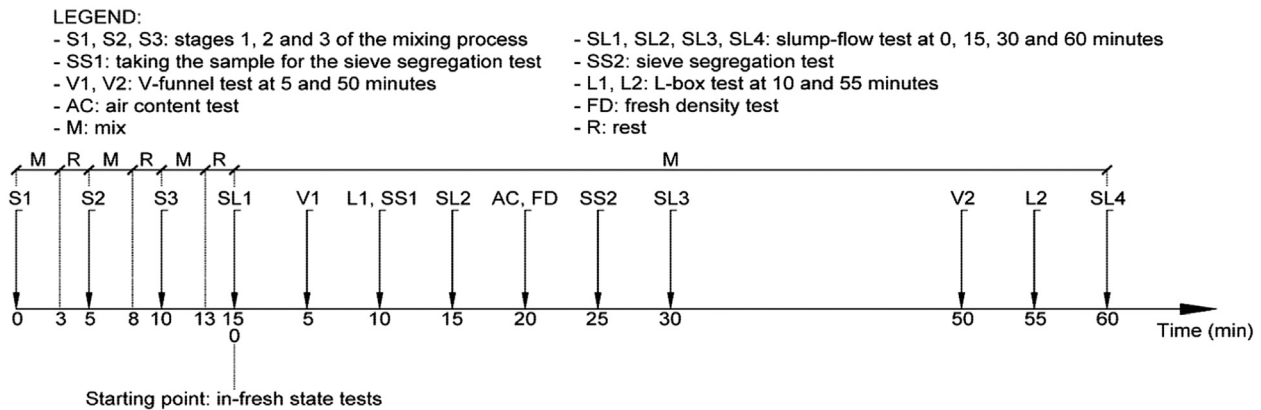
Fig. 2. In-fresh state testing program.

vibration (Santos et al., 2019a). In this test, the SCC is introduced into the Abrams cone, which is subsequently lifted with a vertical movement, leaving the SCC to flow freely onto a stainless-steel plate, described in Fig. 3. The results of this test are the maximum diameter reached by the SCC, known as slump flow, and the time the SCC takes to reach a diameter of 500 mm (t_{500}), which yields a viscosity measurement of the mix. The addition of RCA with the same granulometry as NA usually results in an SCC of higher viscosity and with a lower slump flow (Carro-López et al., 2015),

which can be compensated by adding a larger amount of water or admixtures (González-Taboada et al., 2017a). This test was performed at 0, 15, 30, and 60 min after the mixing process had ended, to study the temporal evolution of the filling ability of SCC.

3.1.1. Slump-flow, spreading

The effects of RCA and cement type on the slump flow were similar in all series, as shown in Fig. 4:

Table 1
Composition of the F mixes (kg/m^3).

	I-0/F	I-50/F	I-100/F	III-0/F	III-50/F	III-100/F
CEM I # CEM III/A	300 # 0			0 # 425		
Ultra-fine limestone powder <0.063 mm	165					
Water	185	210	235	185	210	235
Coarse RCA 4/12.5 mm	530			430		
Fine RCA 0/4 mm	0	505	1010	0	505	1010
Siliceous sand 0/4 mm	1100	550	0	1100	550	0
AD1 # AD2	2.30 # 4.50					

Table 2
Composition of the L mixes (kg/m^3).

	I-0/M	I-50/M	I-100/M	III-0/M	III-50/M	III-100/M
CEM I # CEM III/A	300 # 0			0 # 425		
Limestone fines 0/0.5 mm	335					
Water	185	210	235	185	210	235
Coarse RCA 4/12.5 mm	530			430		
Fine RCA 0/4 mm	0	435	865	0	435	865
Siliceous sand 0/4 mm	940	475	0	940	475	0
AD1 # AD2	2.30 # 4.50					

Table 3
Composition of the R mixes (kg/m^3).

	I-0/R	I-50/R	I-100/R	III-0/R	III-50/R	III-100/R
CEM I # CEM III/A	300 # 0			0 # 425		
RCA 0/0.5 mm	305					
Water	200	220	245	200	220	245
Coarse RCA 4/12.5 mm	530			430		
Fine RCA 0/4 mm	0	435	865	0	435	865
Siliceous sand 0/4 mm	940	475	0	940	475	0
AD1 # AD2	2.30 # 4.50					

- The higher content of fine RCA particles smaller than 0.25 mm in comparison with siliceous sand, caused this by-product to increase the initial slump flow. It therefore compensated the other negative effects of fine RCA, such as its angular shaped particles (Revilla-Cuesta et al., 2020b). However, the high water absorption of the fines hindered the temporal evolution of the slump flow (González-Taboada et al., 2017b), and the slump-flow percentages gradually decreased.

- The initial slump flows of the CEM III mixtures, between 800 and 850 mm, were higher than those of the CEM I mixtures, with values between 750 and 800 mm, due to their higher fineness and lower proportion of coarse RCA. In relation to the slump flows over time, higher relative decreases at 15 and 30 min were noted for the CEM I mixtures. These reductions, between 3% and 10%, were similar to those obtained in SCC with only fine RCA (0% coarse RCA) when limestone aggregate powder was added (Carro-López et al., 2015). Nevertheless, the decreases at 60 min, which averaged between 25 and 35%, were higher when CEM III was used.

The effect of each aggregate powder was different:

- The mixtures produced with CEM I and ultra-fine limestone powder (<0.063 mm) were not very sensitive to the addition of fine RCA (decreases at 60 min of 19.9 and 20.8% for 0 and 100% fine RCA, respectively). They also presented the highest initial slump flow of all the CEM I mixtures. Therefore, the use of good-quality cement and aggregate powder and correct hydration of the aggregates yielded an SCC with a consistent slump-flow evolution over time when adding 100% coarse and fine RCA.

- Initial slump flows similar to those of the F mixes were obtained when adding limestone fines 0/0.5 mm (L mixes), although the slump flow of those mixes decreased less over time. In addition, it was the aggregate powder that showed the best interaction with GGBFS, especially in the short term: the slump flow of mix III-0/L at 15 min (830 mm) was higher than the initial one (810 mm). The addition of the limestone fines produced a concrete with an optimum filling ability, which may also be observed in the initial slump flow of SCC produced with other wastes (Santamaría et al., 2020b).

- The mixes with RCA 0/0.5 mm (R mixes) showed the lowest initial slump flows and the highest percentage decreases, due to the high water absorption of this aggregate powder (Pan et al., 2020). Mixes III-50/R and III-100/R were the only two not to reach at least a SF1 slump-flow class at 60 min.

According to the results, if limestone aggregate powder is used, highly SCC produced with large quantities of alternative materials such as RCA or GGBFS can maintain its self-compactability for up to 60 min after the mixing process. This recycled aggregate SCC can therefore be properly poured on site at distances (in time) of 60 min from the point of manufacture.

3.1.2. Viscosity (t_{500})

Fig. 5 shows the temporal evolution of viscosity determined with the slump-flow test (t_{500}). Although no clear trends may be detected as in the slump flow, some notable aspects are as follows:

- The viscosity of the SCC mixes with CEM I was higher than that of the mixes with CEM III for the same fine RCA content and the same type of aggregate powder. This result validates the use of GGBFS for producing SCC of acceptable initial viscosity, as observed in SCC with 100% NA (Salehi and Mazloom, 2019). However, this alternative binder induced higher relative increases in viscosity over time: 63.6 and 218.2% at 30 and 60 min, respectively, for mix I-0/F, and 75.0 and 325.0% for mix III-0/F.

- The increase in fine RCA content resulted in a higher viscosity at all times, probably due to the rougher surface of its particles. Nevertheless, this increase, at around 40−120%, was lower than the increase in the SCC mixes with only coarse RCA 30 min after

Table 4
Fresh state tests performed: regulations, and SCC classifications.

Criteria	Regulations (EN-Euronorm)	Classification according to EFNARC (2002)
Filling ability, slump flow	EN 12350-8	SF1 (550−650 mm)
		SF2 (650−750 mm)
		SF3 (750−850 mm)
Viscosity according to slump-flow test		VS1 (<2 s)
		VS2 (>2 s)
Viscosity according to V-funnel test	EN 12350-9	VF1 (<8 s)
		VF2 (8−25 s)
Passing ability according to L-box test	EN 12350-10	PA1 (H_1/H_2 > 0.80; 2-bar L-box test)
		PA2 (H_1/H_2 > 0.80; 3-bar L-box test)
Resistance to segregation according to sieve-segregation test	EN 12350-11	SR1 (<20%)
		SR2 (<15%)
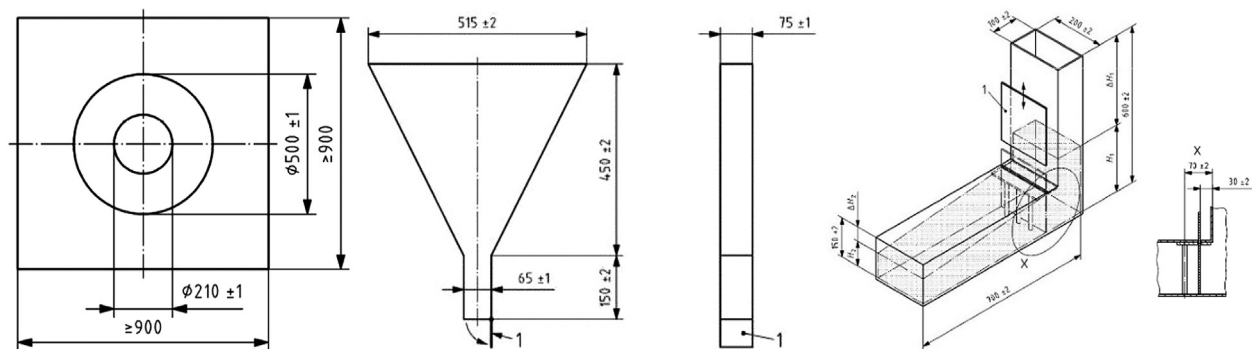
Fig. 3. Scheme of the apparatus used in slump-flow (left), V-funnel (middle), and L-box (right) tests (EN-Euronorm). Dimensions in mm. Number "1" refers to the apparatus gate through which SCC flows.

the mixing process (130−160%), possibly due to the mixing process designed in this study (González-Taboada et al., 2017a).

- The lowest initial viscosity was obtained in the mixes with ultra-fine limestone powder (F mixes), due to its small particle sizes. The worst temporal results were for the R mixes, as the largest percentage decreases in the CEM I mixtures (Fig. 5) were observed following the addition of RCA 0/0.5 mm The highest percentage increase in viscosity was observed in the F mixes with CEM III, due perhaps to the poor interaction between those two materials (Salehi and Mazloom, 2019).

3.1.3. Statistical analysis

The descriptive analyses of the two previous sections presented detailed summaries of each variation in mix composition and its effect on slump flow and viscosity. However, a one-way ANalysis Of VAriance (ANOVA) of these results might determine whether the effect of each factor (each modification in the mix composition: type of cement, fine RCA content, or nature of the aggregate powder) is significant in the results of the slump-flow test compared to the effect of all other factors at each point in time (Cantero et al., 2019). Furthermore, homogeneous groups may be identified, *i.e.*, values of a factor with the same effect on the slump flow and viscosity of the SCC. This analysis was performed at the standard significance level of 5% (Revilla-Cuesta et al., 2020a). The results (Table 5) showed that if the water absorption of the RCA is maximized (a shared objective of both the mix design and the mixing process), its negative effect on the temporal evolution of SCC flowability may not be significant:

- Although the initial slump flow depended on the cement and the fine RCA content, 15 min after the end of the mixing process, it was more dependent on the nature of the aggregate powder.

- The temporal evolution of the viscosity also depended mainly on the aggregate powder in use. Neither the cement, nor the fine RCA content significantly influenced this behavior.

3.1.4. Adjustment model

The statistical model in this section, exclusively devised by the authors of this paper, was used to predict the temporal decrease of the slump flow for each mix (see section 3.1.1).

This model depends on a variable that represents the time lapse from the beginning of the mixing process to the test time: *RWA* (Relative Water Absorption, %). This variable is calculated in equation (1) as the product of the water absorption within 24 h of the fine aggregate (0/4 mm) used to prepare the mix, expressed as a percentage (WA_{24h}, %), and a coefficient, *A*, obtained by statistical fitting of the data from this (see the supplementary data) and other studies (Carro-López et al., 2015; González-Taboada et al., 2017a). Its values, shown in Table 6, reflect the percentage water absorption of the aggregate at each point in time regarding the 24-h water absorption.

$$RWA = A \cdot WA_{24h} \tag{1}$$

The percentage decrease in slump flow (D_{sf}, %) of the mixes may be determined with equation (2). The R^2 coefficient was 94% for CEM I mixtures and 97% for CEM III/A mixtures:

$$D_{sf} = \left(B + \frac{C}{RWA} \right)^2 \quad \text{if CEM I is used}$$

$$D_{sf} = \left(B + C \cdot RWA^2 \right)^2 \quad \text{if CEM III} \Big/ \text{A is used}$$

$$\tag{2}$$

Both formulas depend on coefficients B and C:

(a)

Decrease in slump flow at 15, 30 and 60 minutes (%)

	I-0/F	I-50/F	I-100/F	III-0/F	III-50/F	III-100/F
15 min	- 4.5	- 4.3	- 2.4	- 1.8	- 2.4	- 3.6
30 min	- 8.3	- 9.3	- 11.3	- 5.5	- 7.2	- 10.1
60 min	- 19.9	- 20.4	- 20.8	- 26.1	- 29.9	- 32.5

(b)

Decrease in slump flow at 15, 30 and 60 minutes (%)

	I-0/L	I-50/L	I-100/L	III-0/L	III-50/L	III-100/L
15 min	+ 0.7	- 0.6	- 1.8	+ 1.2	0.0	- 2.3
30 min	- 3.3	- 5.1	- 6.1	- 2.4	- 4.8	- 5.8
60 min	- 13.1	- 15.9	- 22.7	- 21.3	- 25.7	- 31.2

(c)

Decrease in slump flow at 15, 30 and 60 minutes (%)

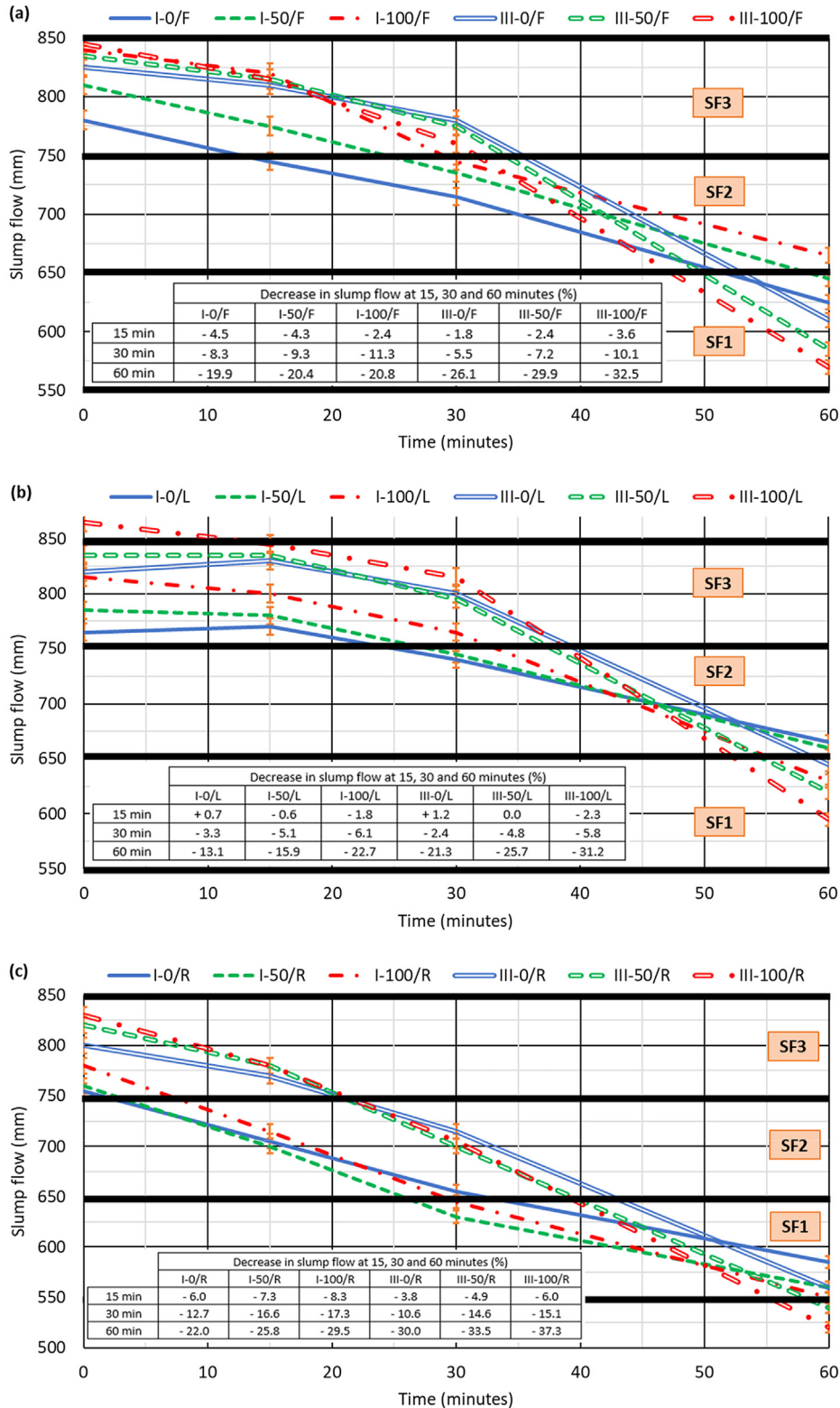|	I-0/R	I-50/R	I-100/R	III-0/R	III-50/R	III-100/R
15 min	- 6.0	- 7.3	- 8.3	- 3.8	- 4.9	- 6.0
30 min	- 12.7	- 16.6	- 17.3	- 10.6	- 14.6	- 15.1
60 min	- 22.0	- 25.8	- 29.5	- 30.0	- 33.5	- 37.3

Fig. 4. Slump-flow evolution over time: (a) F mixes; (b) L mixes; (c) R mixes.

- The formulas to calculate the coefficient B (Table 7) depend on the variable *WAAP* (Water Absorption Aggregate Powder), which is the percentage 24-h water absorption of the aggregate powder. The expression to be used depends on the type of cement and the percentage of fine RCA.

- The other coefficient, C, depends on the variable *RCAP* (Recycled Concrete Aggregate Percentage), which is the fine RCA percentage added to the mix. The formulas, shown in Table 8, vary according to the type of cement and the nature of the aggregate powder.
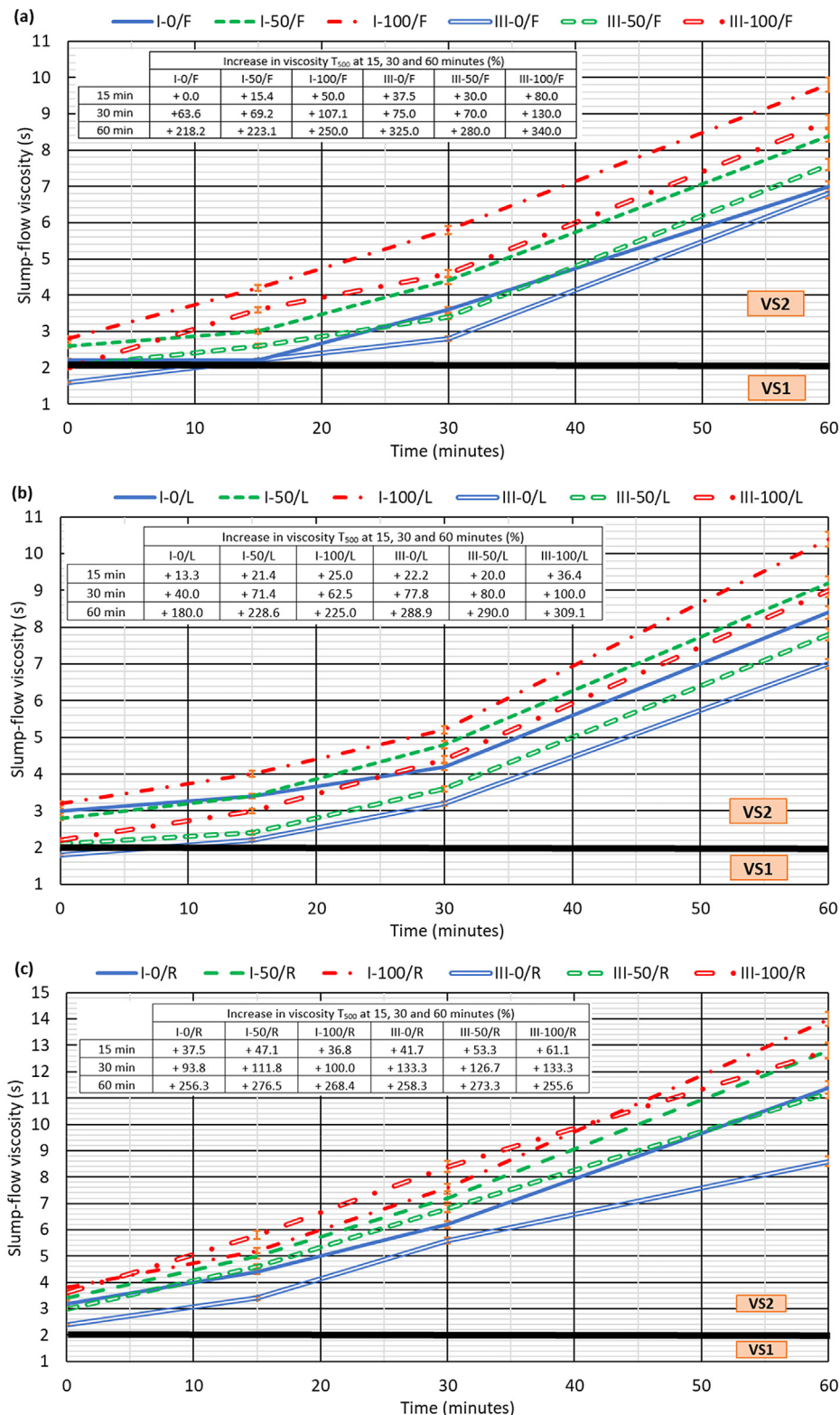
Fig. 5. Viscosity t$_{500}$ evolution over time: (a) F mixes; (b) L mixes; (c) R mixes.

As shown in Fig. 6, a global evaluation of both types of cement mixes revealed that the worst fit was associated with the R mixes, although neither over- nor underestimation exceeded an absolute value of 3%. Furthermore, the data from the few studies that have to date analyzed the temporal flowability of SCC manufactured with only one RCA fraction (Carro-López et al., 2015; González-Taboada et al., 2017a) showed a reasonable fit with the model, as may be observed in Fig. 7. In general, the results of these studies were overestimated at around an absolute value of 2−5%, which suggests that the estimations were on the safe side, although the very

Table 5
One-way ANOVA for slump flow and viscosity (t_{500}).

Condition	Factor	Slump flow		Viscosity	
		P-value	Homogeneous groups	P-value	Homogeneous groups
Time: 0 min	**Cement**	0.0000	None	0.0021	None
	Fine RCA percentage	0.0486	0% and 50%	0.2263	0%, 50% and 100%
			50% and 100%		
	Aggregate powder	0.3780	F, L and R	0.0093	F and L
Time: 15 min	**Cement**	0.0002	None	0.1050	CEM I and CEM III/A
	Fine RCA percentage	0.5592	0%, 50% and 100%	0.1084	0%, 50% and 100%
	Aggregate powder	0.0171	F and L	0.0013	F and L
			L and R		
Time: 30 min	**Cement**	0.0031	None	0.2109	CEM I and CEM III/A
	Fine RCA percentage	0.9500	0%, 50% and 100%	0.0637	0%, 50% and 100%
	Aggregate powder	0.0002	F and L	0.0001	F and L
Time: 60 min	**Cement**	0.0371	None	0.1260	CEM I and CEM III/A
	Fine RCA percentage	0.6228	0%, 50% and 100%	0.2970	0%, 50% and 100%
	Aggregate powder	0.0001	F and L	0.0007	F and L

limited data and studies for the validation of the model must be borne in mind.

This model also reflects the global aspects on which the prediction of the evolution of the slump flow depends, some of which have already been indicated in the statistical analysis (section 3.1.3). Other factors must also be considered to predict the evolution of SCC flowability, although their effects may not be significant with regard to the slump flow of the mixes under study (one-way ANOVA, Table 5). These aspects are:

- Water absorption levels over time, not only of both coarse and fine aggregate as other studies have shown (Santos et al., 2019a), but of all aggregate fractions, including aggregate powder (*RWA* and *WAAP* variables). In this study, RCA was used as a coarse aggregate in all the mixes. If the type of coarse aggregate had differed in each mix, its water absorption should have also been considered (Silva et al., 2018).
- The temporal evolution of the cement rheology (Zuo et al., 2019), as the formula to be used depends on the type of cement that is used.
- The interaction of the cement with all the aggregates added to the mix, especially with the aggregate powder (formulas to calculate coefficients *B* and *C*), which explains the statistical significance of the effect of the aggregate powder on the temporal evolution of the slump flow.

The effect of the last two aspects is clearly shown in the high decrease of slump flow between 30 and 60 min in all the mixes, although aggregate water absorption was fairly low within that period (see the supplementary data).

3.2. Viscosity: V-funnel test

The viscosity characterization of the SCC mixtures was completed with the V-funnel test, according to EN 12350−9 (EN-Euronorm), which was performed at 5 and at 50 min after the end of the mixing process. In this test, the SCC is poured into a V-shaped funnel (see Fig. 3), and the time that SCC takes to flow through the opening of the funnel lid is measured. This test is more demanding than the slump-flow test regarding viscosity, because it forces the SCC to flow in a specific direction (Revilla-Cuesta et al.,

2020c). The results are shown in Fig. 8. Mixes I-0/F, III-0/F, I-0/L, and III-0/L were of VF1 class. Mixes I-100/R and III-100/R (emptying time greater than 25 s) showed no compliance with the recommendations of EFNARC (2002).

The increase in the percentage of fine RCA increased the emptying time, due to the higher segregation within the SCC, which caused a discontinuous and irregular free-fall flow (Santos et al., 2019b). Initial viscosity improved in the CEM III mixes, mainly due to their lower proportion of coarse aggregate, an aspect that conditions this property to a greater extent (Santamaría et al., 2017). Thus, compared to the viscosity of the control mix I-0/F (7.2 s), emptying times increased 172.2% for mix I-100/F (19.6 s), −11.1% for mix III-0/F (6.4 s), and 97.2% for mix III-100/F (14.2 s). The increase was 121.9% for the latter mix with respect to mix III-0/F. These increases were slightly higher than when only one RCA fraction was used: around 85% for 100% coarse RCA (González-Taboada et al., 2017a) and around 110% for 100% fine RCA (Carro-López et al., 2015).

As with the slump-flow test, the L mixes were also the least viscous in the V-funnel test, because the high proportion of particle sizes between 0.25 and 0.50 mm in this aggregate powder resulted in a very compact cement paste that dragged the larger aggregate particles more easily (Danish and Mohan Ganesh, 2015). RCA 0/0.5 mm hindered the dragging of the coarser aggregate particles, due to their higher water absorption, their irregular shape and, especially, their lower density (Carro-López et al., 2015).

The emptying times at 50 min were, on average, 270% higher than at 5 min (Fig. 8a). The effect of fine RCA was more negative than at 5 min and, although the behavior of CEM III improved on the behavior of CEM I, its effect was not as beneficial. CEM III mixtures again showed a greater relative increase in viscosity, which was maximum in the mixtures with 100% fine RCA. Mix III-0/L was the only mix that presented an emptying time that was shorter than 25 s (VF2 class). R mixes experienced an increase in the emptying time that was much higher than the rest of the mixes, and mixes I-100/R and III-100/R even blocked the funnel completely. Increased viscosity of SCC can hinder the pumping process. It therefore appeared reasonable to limit the fine RCA content to 50%, while the use of GGBFS hardly appeared disadvantageous when compared to conventional cement.

Table 6
Values of coefficient A.

Time elapsed since the beginning of the mixing process (min)	5	10	15	30	45	60	75	90
Coefficient A	0.55	0.70	0.75	0.80	0.85	0.88	0.90	0.92

Table 7
Calculation of the coefficient B.

	CEM I	CEM III/A
0% fine RCA	$28.05 - 5.00 \cdot WAAP + 1.17 \cdot WAAP^2 - 0.07 \cdot WAAP^3$	$-13.50 + 3.25 \cdot WAAP - 1.51 \cdot WAAP^2 + 0.14 \cdot WAAP^3$
50% fine RCA	$28.04 - 3.54 \cdot WAAP + 0.81 \cdot WAAP^2 - 0.04 \cdot WAAP^3$	$-12.34 + 2.29 \cdot WAAP - 0.97 \cdot WAAP^2 + 0.09 \cdot WAAP^3$
100% fine RCA	$32.71 - 11.40 \cdot WAAP + 4.65 \cdot WAAP^2 - 0.41 \cdot WAAP^3$	$-13.31 + 2.05 \cdot WAAP - 0.87 \cdot WAAP^2 - 0.08 \cdot WAAP^3$

Table 8
Calculation of the coefficient C.

	CEM I	CEM III/A
Ultra-fine limestone powder	$-4.79 - 1.31 \cdot RCAP - 0.00178 \cdot RCAP^2$	$318.14 - 9.49 \cdot RCAP + 0.06312 \cdot RCAP^2$
Limestone fines 0/0.5 mm	$-4.19 - 1.09 \cdot RCAP - 0.00382 \cdot RCAP^2$	$301.95 - 9.00 \cdot RCAP + 0.05988 \cdot RCAP^2$
RCA 0/0.5 mm	$-5.17 - 1.54 \cdot RCAP - 0.00174 \cdot RCAP^2$	$344.08 - 10.26 \cdot RCAP + 0.06827 \cdot RCAP^2$
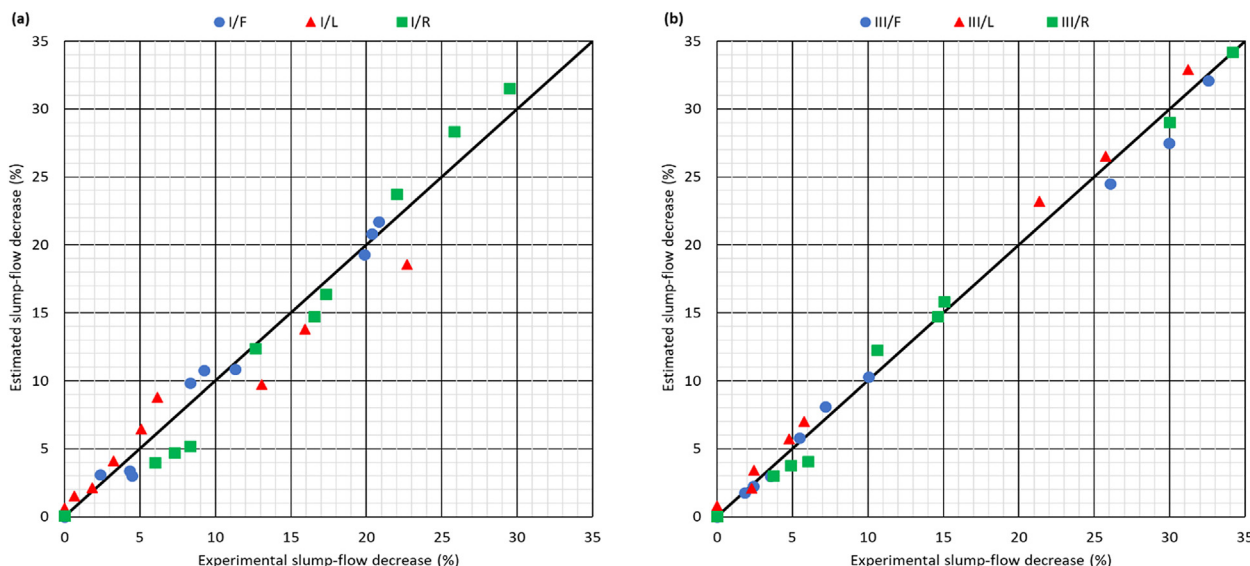
Fig. 6. Relationship between estimated and experimental slump flow: (a) CEM I; (b) CEM III/A.

3.3. Passing ability: 2-bar L-box test

In the L-box test, according to EN 12350−10 (EN-Euronorm), the SCC is poured into the vertical zone of a L-shaped box (Fig. 3). When the gate of the box is opened, the SCC flows into a horizontal zone through bars that simulate concrete reinforcement. The test result, known as the blocking ratio, is the ratio between the height of the SCC mass before the bars and at the end of the horizontal zone. Although SCC flows freely downwards in the V-funnel test and its movement is eventually horizontal in the L-box test, in both tests the SCC is forced to flow through an obstacle under its own weight with no other forces acting upon it. This causes similarities in the results of both tests (Reddy et al., 2020). In this study, the L-box test was performed 10 and 55 min after the end of the mixing process, with similar results to those obtained in the V-funnel test, although there were also some differences, mainly regarding the effect of the fine RCA (see Fig. 9).

- The CEM III mixes yielded better blocking ratios, due to their lower coarse RCA.
- The L mixes showed the best behavior, as the limestone fines 0/0.5 mm created very compact cement pastes exerting an optimal drag force on the coarse aggregate (Santamaría et al., 2020a). In fact, mix III-100/L had the maximum blocking ratio after 10 min, 0.97. The worst results were obtained with RCA 0/0.5 mm due to

its lower density, its rough form, and its high water-absorption levels (Santos et al., 2019b).

- Unlike the V-funnel test, the use of fine RCA 0/4 mm, with a higher content of particles smaller than 0.25 mm compared to siliceous sand, 0/4 mm, created a cement paste with a higher dragging capacity. Its use, therefore, improved the passing ability (blocking ratio of 0.83, 0.86 and 0.91 at 10 min for mixes I-0/F, I-50/F, and I-100/F, respectively). The content of aggregate particles with a size of 0.25−0.50 mm is clearly fundamental to this property, as shown in other studies (Santamaría et al., 2017) and as found when using only coarse RCA (González-Taboada et al., 2017a).

At 55 min, the beneficial effect of CEM III on the passing ability was lower, and its use led to higher relative decreases. The difference in the blocking ratio between the mixes with fine RCA and the mixes with 100% siliceous sand 0/4 mm was lower than at 10 min. Finally, the higher water absorption of RCA 0/0.5 mm explains the highest decrease in the blocking ratio, although limestone aggregate powders showed the worst interaction with GGBFS regarding the relative decrease of this property. According to the EFNARC (2002) recommendations, both F and L mixes would be suitable for the concreting of conventional reinforced concrete elements around 1 h after their manufacture.
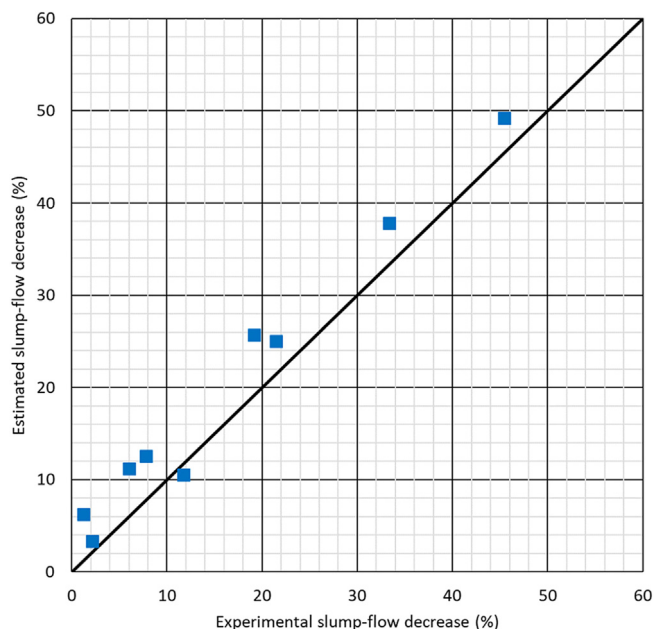
Fig. 7. Validation of the model developed with the data from other studies.

3.4. Sieve segregation

The sieve-segregation test, as per EN 12350−11 (EN-Euronorm), assesses the adhesion of the cementitious matrix to larger aggregate particles (Revilla-Cuesta et al., 2020c). In this test, the SCC is placed on a 5-mm-opening sieve after 15 min of rest, and the amount of mix that passes through it is weighed. The quotient between this mass and the total amount of SCC deposited on the sieve is called sieve segregation. Fig. 10 shows that all mixtures had a SR2 segregation-resistance class; none exceeded 4% sieve segregation. The results were excellent for the SCC of SF3 slump-flow class, which is very sensitive to segregation. This behavior can be explained by the fast loss of flowability of SCC without mixing, thanks to the accurate amount of water added.

The higher segregation of the CEM III mixes was mainly due to their higher proportion of cement paste: the segregation of mix III-0/F was 3.57%, 93.0% higher than the segregation of mix I-0/F (1.85%). The addition of fine RCA reduced the segregation, mainly due to the higher water absorption of this aggregate during the 15 min that the SCC was left to rest (Santos et al., 2019a). The same behavior was found when adding only one RCA fraction (González-Taboada et al., 2017a).

The effect of each aggregate powder mainly depended on its water absorption. The R mixes yielded the best results as they contained the aggregate powder with the highest water absorption levels (sieve segregation around 1% for mixes with CEM I and 1.5% for mixes with CEM III). The segregation of the F and L mixes was similar, although it was slightly better in mixes with limestone fines 0/0.5 mm, due to their larger particle sizes.

3.5. Air content

The air content was determined by the pressure method according to EN 12350−7 (EN-Euronorm). This method consists of introducing the concrete into a micro-compressor and obtaining the value of occluded air as the difference in pressure before and after the valves are opened. The mixtures in this study were tested without vibration after having been placed inside the micro-compressor, thus reproducing the optimal placement of SCC

(EFNARC, 2002). The addition of high quantities of plasticizer to achieve self-compactability (Huang et al., 2018) and the high RCA content (Revilla-Cuesta et al., 2020c) resulted in a high air content in all the mixes, as shown in Fig. 11: the air content was higher than 4% in 16 of the 18 mixes under study.

Since RCA is more porous than siliceous sand due to the presence of adhered mortar, the air content increased with the addition of fine RCA (Silva et al., 2018). On the other hand, as a higher initial flowability was achieved in the mixes made with CEM III, they had a more liquid cement paste that facilitated the expulsion of air (Santamaría et al., 2020b). Their air content was therefore lower (for example, the air content of mixes I-100/L and III-100/L was 5.3 and 4.4%, respectively). So, the increased air content of the mixes after adding 45% GGBFS (Salehi and Mazloom, 2019) was compensated by the increased flowability of the SCC.

The larger particle sizes of the aggregate powder hindered the expulsion of air (Matar and Barhoun, 2020). The mixes with ultra-fine limestone powder showed the best results, though very close to those of the L mixes (air content of 3.9 and 4.0% for mixes I-0/F and I-0/L). The high micro-porosity of RCA 0/0.5 mm was very negative: the air content of almost all the R mixes was over 5% (maximum value in mix I-100/R, 6.6%).

3.6. Fresh density

The fresh density of concrete is determined by placing the fresh concrete in a recipient with a measured volume, as specified in EN 12350−6 (EN-Euronorm). The quotient between the specified concrete mass placed in the recipient and the full volume of the recipient represents the value of this property. The density of the components conditioned the fresh density of the concrete (Fig. 12). Thus, fresh density increased with the higher cement content of CEM III that is of higher density than the aggregate, and decreased when fine RCA, less dense than fine NA, was added (Fiol et al., 2018). The densest aggregate powder, limestone fines 0/0.5 mm, produced the densest mixtures (Rebello et al., 2019).

However, the density of the mixes was also very sensitive to variations in the air content, as shown in Fig. 13, which reflects the close relation between a higher air content and a lower SCC fresh density. In consequence, non-uniform variations in density across all mixture series occurred when a certain percentage of fine RCA was added, a trend also observed in vibrated concrete (Silva et al., 2018).

4. Results and discussion: hardened behavior

In addition to optimum flowability, the hardened behavior of SCC must also be reasonable (Revilla-Cuesta et al., 2020c). Accordingly, the hardened density and 28-day compressive strength of the mixtures were also evaluated on a set of $10 \times 10 \times 10$-cm cubic specimens. These properties, along with the thermal properties, are useful for defining the validity of an SCC to be used from a functional point of view. A first approach to this thermal behavior is shown in a previous study of the authors (Revilla-Cuesta et al., 2020b). In this study, the thermal deformability of the SCC made with RCA was evaluated under both positive and negative cyclical temperature variations. The thermal strain was continuously measured using strain gauges. It was found that the use of 100% fine RCA increased the thermal strain by 10%, while this increase was 26% for a full replacement of coarse NA with RCA. Therefore, the use of RCA, especially of the coarse fraction, implies higher stresses in SCC due to temperature changes, which should be considered when RCA is used in structural SCC.
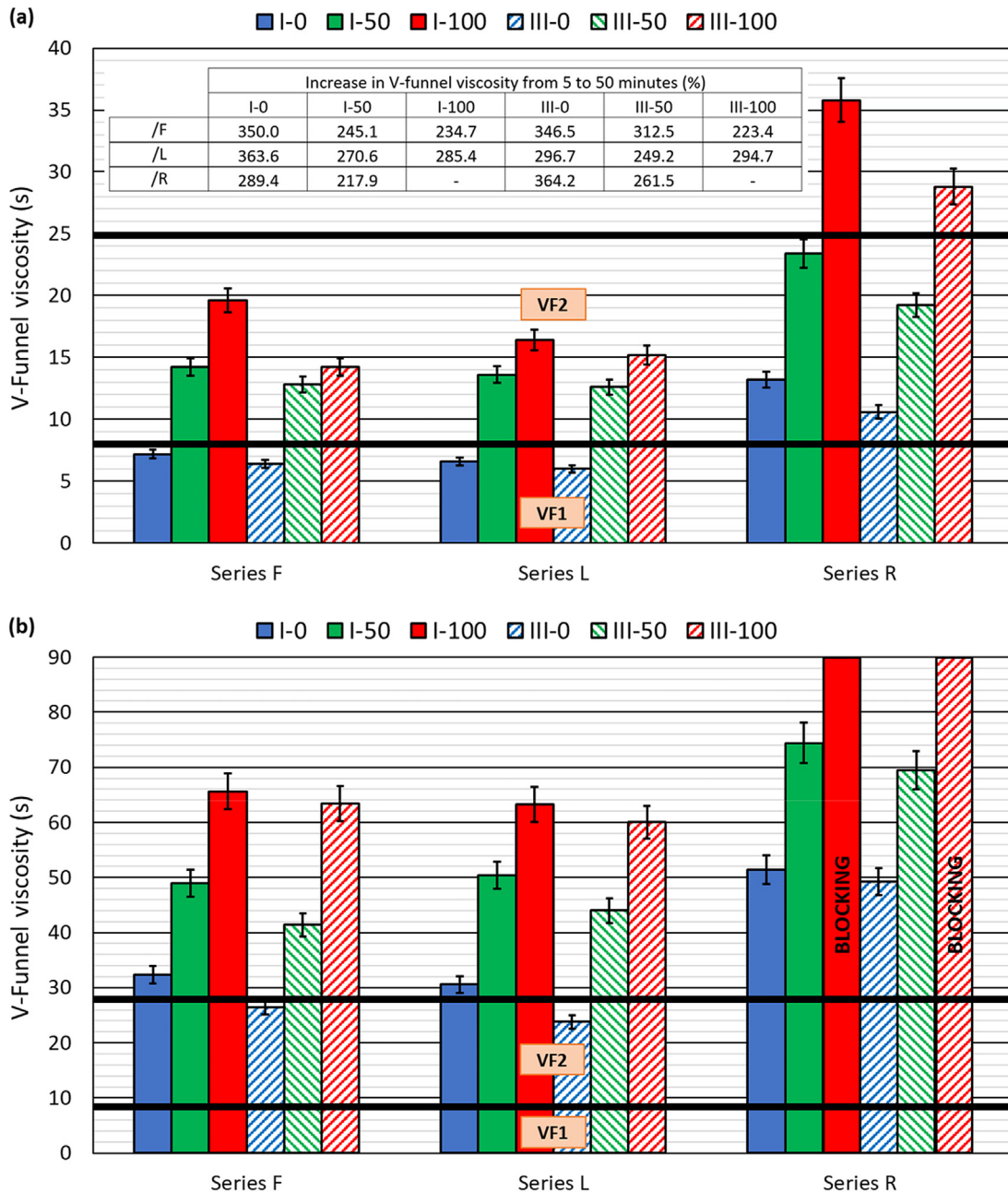
(a)

		Increase in V-funnel viscosity from 5 to 50 minutes (%)					
		I-0	I-50	I-100	III-0	III-50	III-100
	/F	350.0	245.1	234.7	346.5	312.5	223.4
	/L	363.6	270.6	285.4	296.7	249.2	294.7
	/R	289.4	217.9	-	364.2	261.5	-

(b)

Fig. 8. Results of V-Funnel test: (a) at 5 min; (b) at 50 min..

4.1. Hardened density

Among the different concrete density tests of EN 12390−7 (EN-Euronorm), in this study the real density was determined, in terms of the hydrostatic equilibrium or weight difference. The hardened density was lower than the fresh density, due to the evaporation of the water released in a delayed way from the aggregate after mixing or not absorbed by the mix components (Sainz-Aja et al., 2019). Fig. 14 shows the results of real density (and the decrease in comparison with the fresh density) of all the mixes. The results reproduced the fresh density behavior (section 3.6): the use of CEM III increased the density, and the addition of fine RCA and RCA 0/0.5 mm, of lower density than fine NA and limestone aggregate powder, respectively, reduced it.

The release of water from the aggregate and the amount of water not absorbed in the mix components conditioned the variation between the real and the fresh densities. On the one hand, the high water absorption of RCA led to a higher delayed release of water after mixing, which increased the water evaporation, the mass loss, and the density reduction (Gonzalez-Corominas and Etxeberria, 2016). On the other, the use of fine RCA and aggregate powders with irregular shapes, such as limestone fines 0/0.5 mm and RCA 0/0.5 mm, also augmented this decrease in density. The distribution of water within the concrete was less uniform when using these aggregates, resulting in higher water evaporation (Revilla-Cuesta et al., 2020a). Finally, CEM III, which produced more fluid mixes, also slightly increased this density variation.
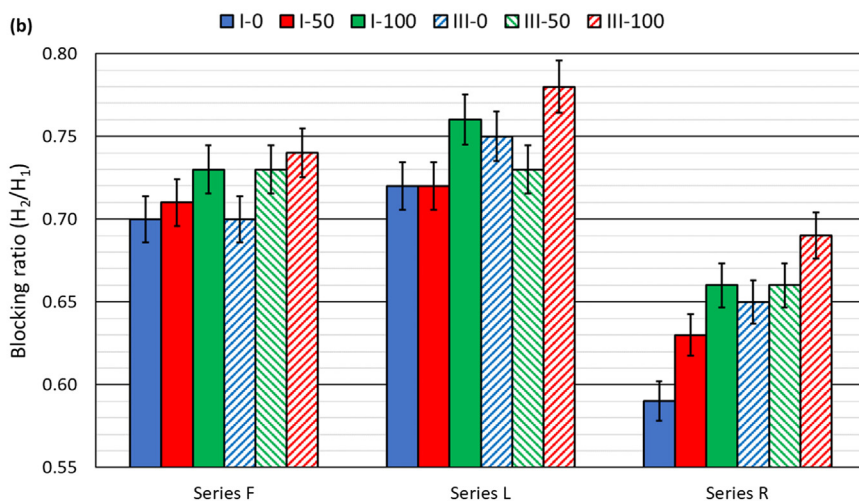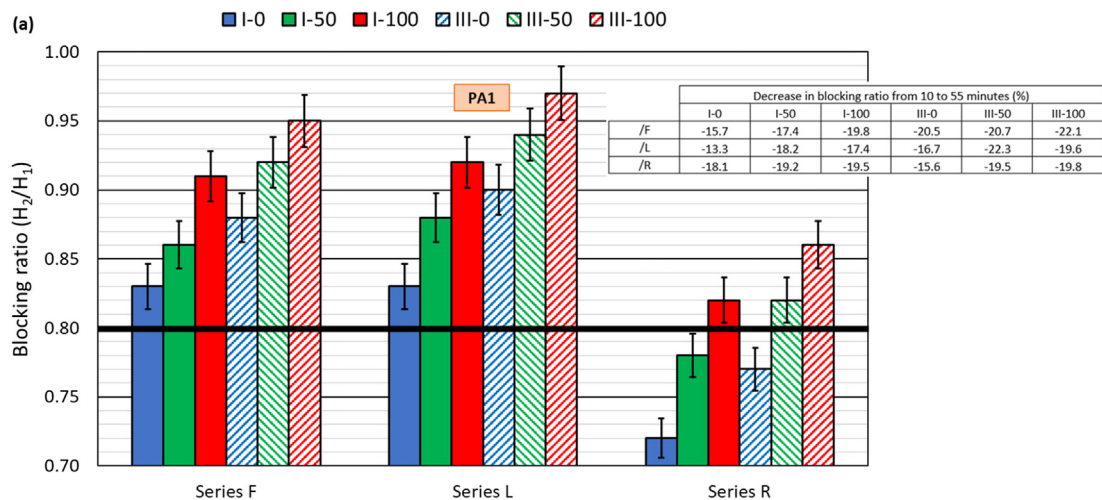
(a)

Legend: ■ I-0 ■ I-50 ■ I-100 ▨ III-0 ▨ III-50 ▨ III-100

PA1

Decrease in blocking ratio from 10 to 55 minutes (%)						
	I-0	I-50	I-100	III-0	III-50	III-100
/F	-15.7	-17.4	-19.8	-20.5	-20.7	-22.1
/L	-13.3	-18.2	-17.4	-16.7	-22.3	-19.6
/R	-18.1	-19.2	-19.5	-15.6	-19.5	-19.8

Y-axis: Blocking ratio (H_2/H_1), range 0.70 to 1.00

X-axis: Series F, Series L, Series R

(b)

Legend: ■ I-0 ■ I-50 ■ I-100 ▨ III-0 ▨ III-50 ▨ III-100

Y-axis: Blocking ratio (H_2/H_1), range 0.55 to 0.80

X-axis: Series F, Series L, Series R

Fig. 9. Results of 2-bar L-box test: (a) at 10 min; (b) at 55 min.

Legend: ■ I-0 ■ I-50 ■ I-100 ▨ III-0 ▨ III-50 ▨ III-100

SR2

Y-axis: Sieve segregation (%), range 0.0 to 4.0

X-axis: Series F, Series L, Series R
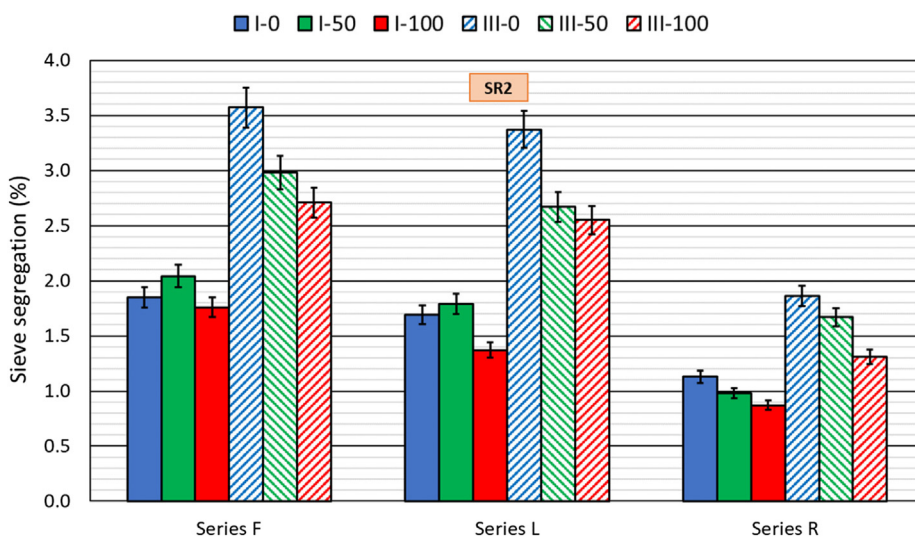
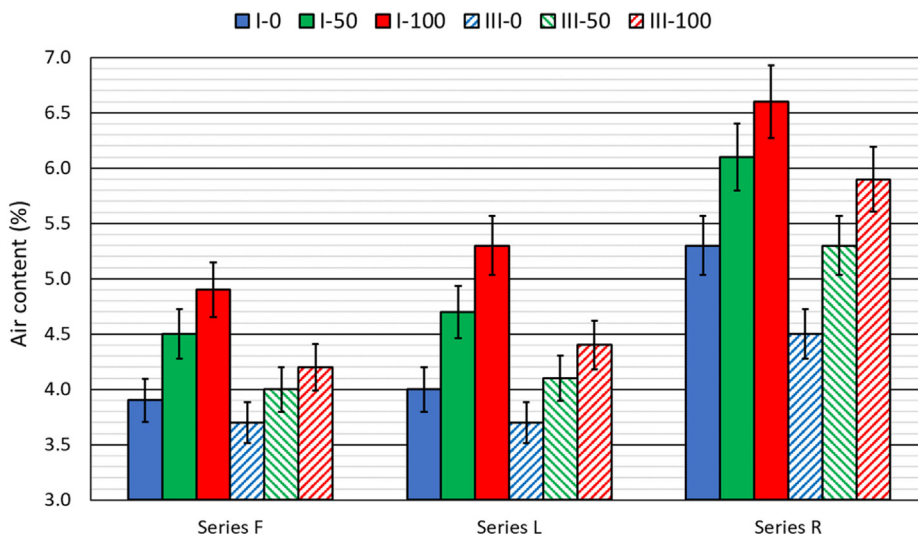**Fig. 10.** Results of sieve-segregation test.
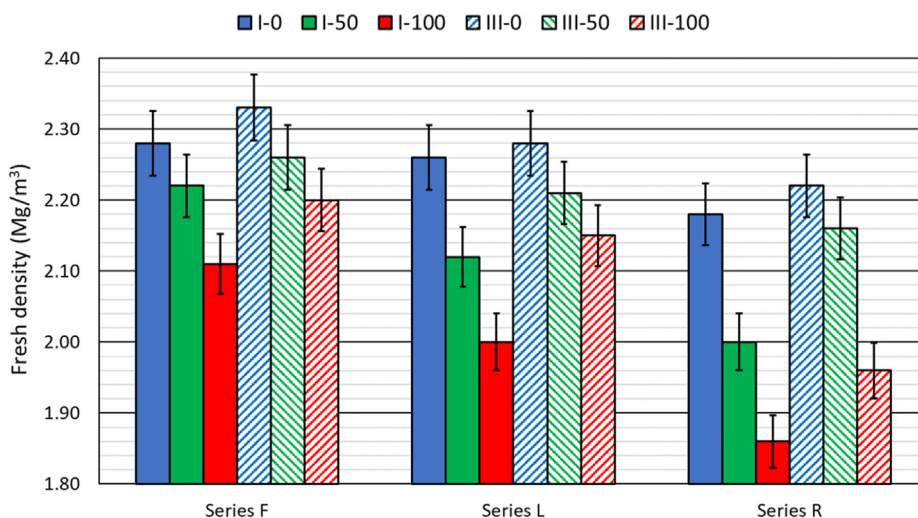
Fig. 11. Results of air content test.

Fig. 12. Fresh density of the mixes.

4.2. Compressive strength

The compressive strength of concrete, as per EN 12390−3 (EN-Euronorm), is determined by applying a compressive force to a standardized specimen at a rate between 0.4 and 0.8 MPa/s. The use of RCA decreases the compressive strength of the concrete (Silva et al., 2015), although its addition can still produce high-strength SCC (Revilla-Cuesta et al., 2020c), as shown in some of the mixes in this study (third column of Table 10). Therefore, some of the SCC mixes might also be valid for structural use from the point of view of their strength, thus increasing the sustainability of commonly used SCC. Some relevant aspects were observed:

- The higher cement content of the CEM III mixes balanced the lower strength expected from using GGBFS (Yang et al., 2019), and even increased the strength: mixes III-0/F and III-0/L (55 and 62 MPa respectively) had 9.2 and 17.0% higher strengths than mixes I-0/F and I-0/L (50.5 and 53 MPa), respectively.
- The addition of fine RCA instead of siliceous sand decreased the compressive strength, mainly when using CEM I. The decrease between mixes with 0 and 50% fine RCA was lower than between mixes with 50 and 100% fine RCA: the respective strengths of mixes I-50/F and I-100/F were 8.2 and 35.9% lower than that of mix I-0/F. This non-proportional decrease was due to the filler effect of the high fines content of fine RCA, which was all the more outstanding when adding low or medium contents of RCA (Vinay Kumar et al., 2017).
- Limestone fines 0/0.5 mm provided mixtures of higher strength than ultra-fine limestone powder. Mixes III-0/L and III-50/L exceeded compressive strengths of 55 MPa. The R mixes presented the lowest strength (average loss close to 20%), although the usual value of 30 MPa when using 300 kg/m³ of cement was achieved in all mixes except in mix I-100/R (lowest density, highest air content).

Fragments of mix III-50/L were examined under a Scanning Electron Microscope (SEM) to complete the analysis, as shown in Fig. 15. A micrometer-scale siliceous sand particle belonging to an RCA particle can be observed. This particle of siliceous sand and the mortar adhering to it, of a darker color than the new cementious
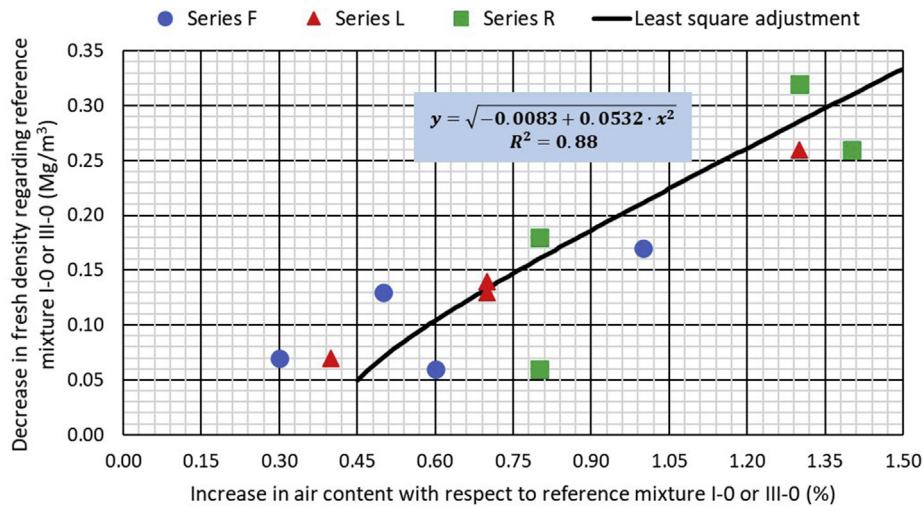
Fig. 13. Relationship between air content increase and fresh density decrease.

matrix, were broken during the test. Good adhesion between the RCA and the cementitious matrix in the interfacial transition zones was detected as the aggregate broke, reflecting the high compressive strength of this mix.

The Spanish Structural Concrete Code, EHE-08 (2010), and Eurocode 2 (EC-2, 2010) likewise define lightweight concrete as concrete with a density between 1.2 and 2.0 Mg/m³ and a minimum compressive strength of 25 MPa. Mixes I-100/L and III-100/R fulfilled these requirements, and could be treated as lightweight concretes, highlighting a potential field of application for RCA (Wongsa et al., 2020).

5. Results and discussion: carbon footprint

The calculation of the carbon footprint of the mixes was limited to the contributions of the different raw materials used in their manufacture. The production and transport of concrete can be considered similar in all mixes. Therefore, these factors were omitted, as they are irrelevant for a comparative analysis of the carbon footprint (Song et al., 2019). Table 9 shows the carbon footprint of the raw materials of the SCC mixes under study, which were obtained through a life cycle assessment performed by Yang et al. (2015) for the binders, admixtures, and water, Rebello et al. (2019) for the aggregate powders, and Hossain et al. (2016) for the NA and RCA.

The carbon footprints (fourth column of Table 10) were calculated from the mix design (section 2.2) and the data in Table 9. These values show that the use of coarse RCA reduced the carbon footprint by 0.93%, while the decrease due to fine RCA was only 0.50−0.60%. In contrast, neither the addition of limestone fines 0/0.5 mm nor RCA 0/0.5 mm in substitution of ultra-fine limestone powder notably reduced the carbon footprint, because those additions also required higher amounts of aggregate powder to be added to the mix. Nevertheless, the high GGBFS content of CEM III/A reduced the carbon footprint by 19.5%, thereby increasing the sustainability of SCC more than any other alternative material.
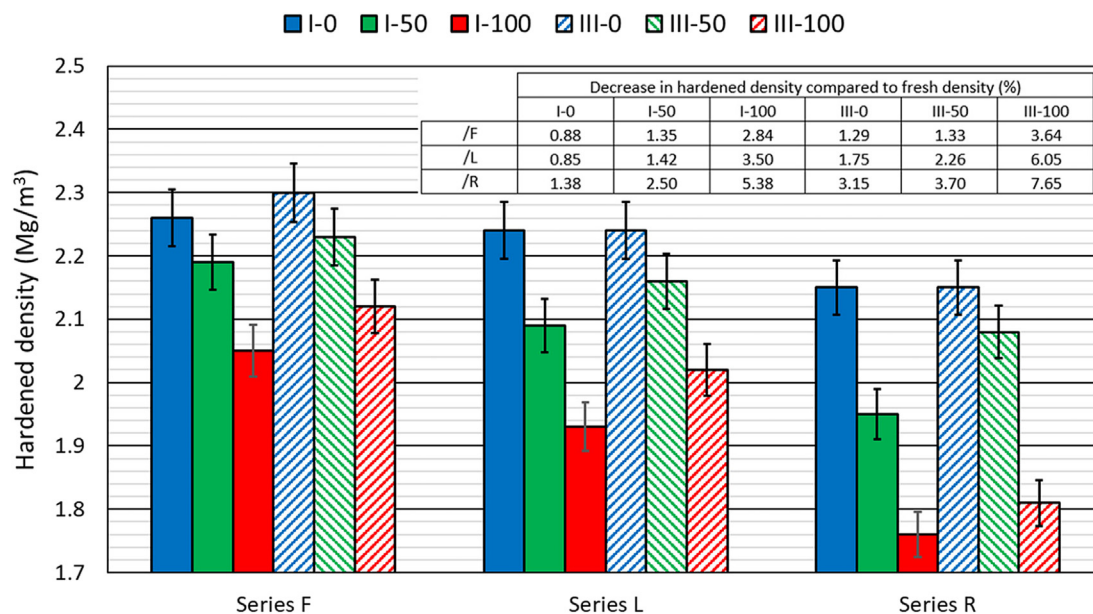

Fig. 14. Hardened density of the mixes and their lower real density in comparison with their fresh density.

Table 9
Carbon footprint of raw materials.

Material	Carbon footprint (kg CO_2 eq/kg)	References considered
CEM I	0.9310	Yang et al. (2015)
GGBFS	0.0265	
Water	0.0002	
Admixtures	0.0005	
Ultra-fine limestone powder	0.0157	Rebello et al. (2019)
Limestone fines 0/0.5 mm	0.0069	
RCA 0/0.5 mm	0.0033	
Coarse NA 4/12.5 mm	0.0075	Hossain et al. (2016)
Coarse RCA 4/12.5 mm	0.0030	
Siliceous sand 0/4 mm	0.0026	
Fine RCA 0/4 mm	0.0011	

Table 10
Global overview of SCC mixes. Choice of the best mix.

Mix	Loss of flowability (slump flow) at 60 min (%)	Compressive strength [a] (MPa)	Carbon footprint [b] (kg CO_2 eq/m³)	Ranking according to TOPSIS algorithm
I-0/F	- 19.9	50.5 ± 1.9	286.4 (−0.93)	5
I-50/F	- 20.4	46.3 ± 1.2	285.5 (−1.23)	7
I-100/F	- 20.8	32.3 ± 3.6	284.6 (−1.53)	11
III-0/F	- 26.1	55.1 ± 3.2	230.0 (−20.43)	6
III-50/F	- 29.9	47.7 ± 3.8	229.1 (−20.73)	9
III-100/F	- 32.5	37.1 ± 2.3	228.3 (−21.03)	16
I-0/L	- 13.1	53.0 ± 2.4	285.7 (−1.17)	3
I-50/L	- 15.9	50.5 ± 1.6	285.0 (−1.42)	4
I-100/L	- 22.7	34.0 ± 2.3	284.2 (−1.68)	13
III-0/L	- 21.3	62.0 ± 1.2	229.3 (−20.67)	1
III-50/L	- 25.7	59.8 ± 3.1	228.6 (−20.92)	2
III-100/L	- 31.2	43.9 ± 1.6	227.8 (−21.19)	12
I-0/R	- 22.0	42.3 ± 2.4	284.4 (−1.62)	8
I-50/R	−25.8	34.5 ± 0.7	283.7 (−1.87)	14
I-100/R	- 29.5	19.0 ± 4.0	282.9 (−2.13)	18
III-0/R	- 30.0	45.9 ± 2.9	228.0 (−21.12)	10
III-50/R	- 33.5	39.6 ± 2.2	227.3 (−21.38)	15
III-100/R	- 37.3	31.8 ± 3.5	226.5 (−21.64)	17

[a] Mean value and standard deviation.
[b] The percentage decreases of the carbon footprint regarding conventional highly SCC (CEM I, 100% NA, and ultra-fine limestone powder) are shown in brackets.

6. Global overview

Table 10 summarizes the most relevant aspects of the mixtures. As indicated in previous sections, the best temporal conservation was obtained in mixes produced with CEM I, although they had lower compressive strengths and higher carbon footprints. The use of up to 50% fine RCA yielded adequate results, while limestone fines 0/0.5 mm were the aggregate powder with the best performance. These three criteria (loss of flowability, compressive strength, and carbon footprint), all with the same weight, were used to determine the best mix through a multi-criteria analysis. The TOPSIS (Technique for Order Preference by Similarity to Ideal Solution) algorithm was chosen, because it is often used for these sorts of problems. Rashid et al. (2020) described its implementation process in their study. Mixes III-0/L and III-50/L had the best ranking according to this analysis (Table 10), which demonstrates the suitability of GGBFS and 50% fine RCA to produce sustainable highly SCC.

7. Conclusions

The effect of the simultaneous addition of different types of waste on the temporal flowability of Self-Compacting Concrete (SCC) has been evaluated in this paper. More specifically, the use of Ground Granulated Blast Furnace Slag (GGBFS) and large amounts of both coarse and fine Recycled Concrete Aggregate (RCA), as well as different types of aggregate powder have all been analyzed. Through 18 SCC mixtures with different composition, it has been demonstrated that if the mix design is adapted to the particular characteristics of the components of the SCC, a sustainable SCC may be obtained with a high initial flowability, an SF3 slump-flow class (EFNARC, 2002), and at least an SF1 slump-flow class 60 min after the end of the mixing process. Nevertheless, other relevant conclusions can be drawn from the aspects addressed in the article:

- Both GGBFS and fine RCA improved the filling ability at the initial moment, although hindered its temporal conservation. The use of limestone fines 0/0.5 mm allowed obtaining SCC with a better performance in the fresh state over time than conventional ultra-fine limestone powder.
- A statistical adjustment based on the aggregates' water absorption (coarse, fine, and aggregate powder) allowed accurately predicting the temporal decrease of flowability of SCC. This statistical analysis also showed that this temporal conservation depended on the rheology of the cement, and the interaction between the type of cement and the aggregate added to the mix. An optimal hydration of the RCA during the mixing process led this waste not to condition the slump flow of SCC.
- The effect of the different components on the flow of SCC depended on the type of flow imposed. In free-fall flow (V-funnel test), the addition of fine RCA and aggregate powder of larger particle sizes favored a segregated and discontinuous flow. On the other hand, in horizontal flow (L-box test), the increase in the fines content following the addition of fine RCA to SCC mixes improved their passing ability. The lower coarse aggregate content of CEM III mixtures improved both properties.
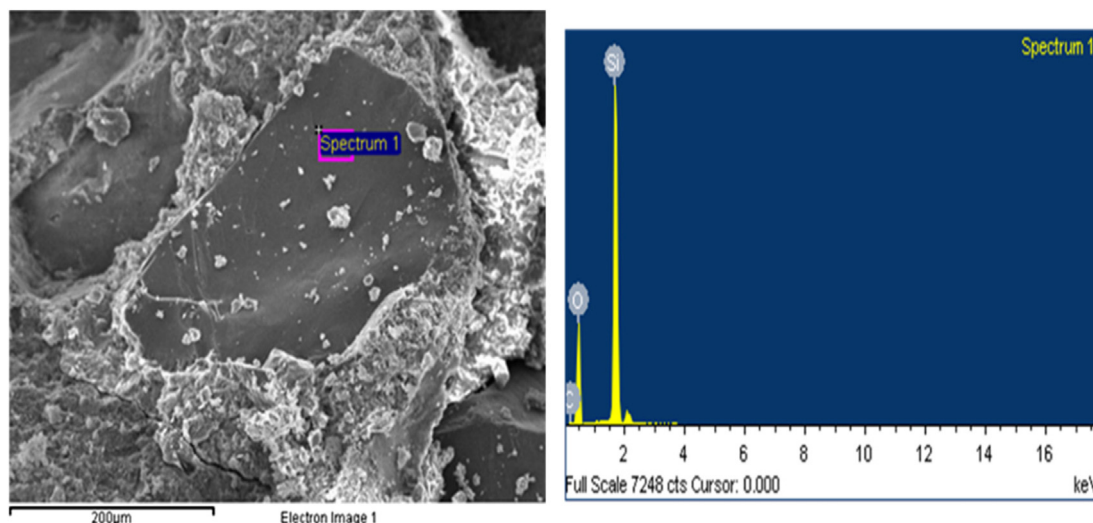
Fig. 15. SEM analysis of mix III-50/L.

Regardless of the mix composition, the temporal conservation of viscosity and passing ability was poor.

- The addition of any RCA fraction increased the air content of the mixtures. An increase in the flowability of the mix without increasing its admixture or water content allowed reducing this increase of air content, although it caused a higher decrease of density from the fresh to the hardened state.

Overall, the mixes with CEM III/A, 100% coarse RCA, 50% fine RCA, and limestone fines 0/0.5 mm demonstrated the best global behavior (flowability, compressive strength, and carbon footprint) according to the multi-criteria analysis. These results have underlined the feasibility of using these components to produce SCC that can be placed on site up to 60 min after the mixing process, which represents a significant advance for the use of recycled aggregate SCC. Nevertheless, further detailed study of their mechanical and thermal behavior in the hardened state is still required to guarantee its successful use.

CRediT authorship contribution statement

Víctor Revilla-Cuesta: Investigation, Methodology, Data curation, Formal analysis, Software, Writing − original draft. **Marta Skaf:** Conceptualization, Investigation, Formal analysis, Project administration, Writing − review & editing. **Amaia Santamaría:** Investigation, Software, Formal analysis, Visualization, Validation. **Jorge J. Hernández-Bagaces:** Investigation, Data curation, Formal analysis, Software. **Vanesa Ortega-López:** Conceptualization, Methodology, Project administration, Funding acquisition, Resources, Writing − review & editing, Supervision.

Declaration of competing interest

The authors declare that they have no known competing financial interests or personal relationships that could have appeared to influence the work reported in this paper.

Acknowledgements

Appendix A. Supplementary data

Supplementary data to this article can be found online at https://doi.org/10.1016/j.jclepro.2021.126890.

References

Abdollahnejad, Z., Luukkonen, T., Mastali, M., Giosue, C., Favoni, O., Ruello, M.L., Kinnunen, P., Illikainen, M., 2020. Microstructural analysis and strength development of one-Part Alkali-activated slag/ceramic binders under different curing regimes. Waste Biomass Valoris 11 (6), 3081−3096. https://doi.org/10.1007/s12649-019-00626-9.

Anefa, 2019. Sectorial Economic Progress Reports.

Cantero, B., Sáez del Bosque, I.F., Matías, A., Sánchez de Rojas, M.I., Medina, C., 2019. Inclusion of construction and demolition waste as a coarse aggregate and a cement addition in structural concrete design. Arch. Civ. Mech. Eng. 19 (4), 1338−1352. https://doi.org/10.1016/j.acme.2019.08.004.

Carro-López, D., González-Fonteboa, B., De Brito, J., Martínez-Abella, F., González-Taboada, I., Silva, P., 2015. Study of the rheology of self-compacting concrete with fine recycled concrete aggregates. Construct. Build. Mater. 96, 491−501. https://doi.org/10.1016/j.conbuildmat.2015.08.091.

Dai, J., Wang, Q., Xie, C., Xue, Y., Duan, Y., Cui, X., 2019. The effect of fineness on the hydration activity index of ground granulated blast furnace slag. Materials 12 (18), 2984. https://doi.org/10.3390/ma12182984.

Danish, P., Mohan Ganesh, G., 2015. Study on self compacting concrete: a state-of-art-of-review. Int. J. Appl. Eng. Res. 10 (93 Special issue), 74−78.

Du, Y.J., Wu, J., Bo, Y.L., Jiang, N.J., 2020. Effects of acid rain on physical, mechanical and chemical properties of GGBS−MgO-solidified/stabilized Pb-contaminated clayey soil. Acta Geotech 15 (4), 923−932. https://doi.org/10.1007/s11440-019-00793-y.

EC-2, 2010. Eurocode 2: Design of Concrete Structures. Part 1-1: General Rules and Rules for Buildings. CEN (European Committee for Standardization).

EFNARC, 2002. Specification Guidelines for Self-Compacting Concrete. European Federation of National Associations Representing producers and applicators of specialist building products for Concrete.

EHE-08, 2010. Structural Concrete Regulations (In Spanish). Ministry of Infraestructures, Spanish Government.

Elahi, M.M.A., Hossain, M.M., Karim, M.R., Zain, M.F.M., Shearer, C., 2020. A review on alkali-activated binders: materials composition and fresh properties of concrete. Construct. Build. Mater. 260, 119788. https://doi.org/10.1016/j.conbuildmat.2020.119788.

EN-Euronorm, Rue de stassart, 36. Belgium-1050 Brussels, European Committee for Standardization.

ERMCO, 2019. Ready-mixed Concrete Industry Statistics. European Ready-Mixed Concrete Organization.

Eurostat, 2019. Waste Statistics.

Fiol, F., Thomas, C., Muñoz, C., Ortega-López, V., Manso, J.M., 2018. The influence of recycled aggregates from precast elements on the mechanical properties of structural self-compacting concrete. Construct. Build. Mater. 182, 309−323. https://doi.org/10.1016/j.conbuildmat.2018.06.132.

Gonzalez-Corominas, A., Etxeberria, M., 2016. Effects of using recycled concrete aggregates on the shrinkage of high performance concrete. Construct. Build. Mater. 115, 32−41. https://doi.org/10.1016/j.conbuildmat.2016.04.031.

Gonzalez-Corominas, A., Etxeberria, M., Poon, C.S., 2017. Influence of the quality of recycled aggregates on the mechanical and durability properties of high performance concrete. Waste Biomass Valoris 8 (5), 1421−1432. https://doi.org/10.1007/s12649-016-9637-7.

González-Taboada, I., González-Fonteboa, B., Eiras-López, J., Rojo-López, G., 2017a. Tools for the study of self-compacting recycled concrete fresh behaviour: workability and rheology. J. Clean. Prod. 156, 1−18. https://doi.org/10.1016/j.jclepro.2017.04.045.

González-Taboada, I., González-Fonteboa, B., Martínez-Abella, F., Seara-Paz, S., 2017b. Analysis of rheological behaviour of self-compacting concrete made with recycled aggregates. Construct. Build. Mater. 157, 18−25. https://doi.org/10.1016/j.conbuildmat.2017.09.076.

Güneyisi, E., Gesoğlu, M., Algin, Z., Yazici, H., 2014. Effect of surface treatment methods on the properties of self-compacting concrete with recycled aggregates. Construct. Build. Mater. 64, 172−183. https://doi.org/10.1016/j.conbuildmat.2014.04.090.

Gupta, N., Siddique, R., Belarbi, R., 2020. Sustainable and greener self-compacting concrete incorporating industrial by-products: a review. J. Clean. Prod. 284, 124803. https://doi.org/10.1016/j.jclepro.2020.124803.

Hossain, M.U., Poon, C.S., Lo, I.M.C., Cheng, J.C.P., 2016. Comparative environmental evaluation of aggregate production from recycled waste materials and virgin sources by LCA. Resour. Conserv. Recycl. 109, 67−77. https://doi.org/10.1016/j.resconrec.2016.02.009.

Huang, F., Li, H., Yi, Z., Wang, Z., Xie, Y., 2018. The rheological properties of self-compacting concrete containing superplasticizer and air-entraining agent. Construct. Build. Mater. 166, 833−838. https://doi.org/10.1016/j.conbuildmat.2018.01.169.

Khan, A.R., Fareed, S., Khan, M.S., 2019. Use of recycled concrete aggregates in structural concrete. Sustain. Constr. Mater. Technol. 2.

Maddalena, R., Roberts, J.J., Hamilton, A., 2018. Can Portland cement be replaced by low-carbon alternative materials? A study on the thermal properties and carbon emissions of innovative cements. J. Clean. Prod. 186, 933−942. https://doi.org/10.1016/j.jclepro.2018.02.138.

Matar, P., Barhoun, J., 2020. Effects of waterproofing admixture on the compressive strength and permeability of recycled aggregate concrete. J. Build. Eng. 32, 101521. https://doi.org/10.1016/j.jobe.2020.101521.

Ouchi, M., Hibino, M., Sugamata, T., Okamura, H., 2000. Quantitative evaluation method for the effect of superplasticizer in self-compacting concrete. Trans. Jpn. Concr. Inst. 22, 15−20.

Pacheco, J., Polder, R.B., 2016. Critical chloride concentrations in reinforced concrete specimens with ordinary Portland and blast furnace slag cement. Heron 61 (2), 99−119.

Pan, S., Chen, D., Chen, X., Ge, G., Su, D., Liu, C., 2020. Experimental study on the workability and stability of steel slag self-compacting concrete. Appl. Sci. 10 (4), 1291. https://doi.org/10.3390/app10041291.

Parron-Rubio, M.E., Perez-García, F., Gonzalez-Herrera, A., Rubio-Cintas, M.D., 2018. Concrete properties comparison when substituting a 25% cement with slag from different provenances. Materials 11 (6), 1029. https://doi.org/10.3390/ma11061029.

Rashid, K., Rehman, M.U., de Brito, J., Ghafoor, H., 2020. Multi-criteria optimization of recycled aggregate concrete mixes. J. Clean. Prod. 276, 124316. https://doi.org/10.1016/j.jclepro.2020.124316.

Rebello, T.A., Zulcão, R., Calmon, J.L., Gonçalves, R.F., 2019. Comparative life cycle assessment of ornamental stone processing waste recycling, sand, clay and limestone filler. Waste Manag. Res. 37 (2), 186−195. https://doi.org/10.1177/0734242X18819976.

Reddy, A.S., Kumar, P.R., Raj, P.A., 2020. Development of sustainable performance index (SPI) for self-compacting concretes. J. Build. Eng. 27, 100974. https://doi.org/10.1016/j.jobe.2019.100974.

Revilla-Cuesta, V., Ortega-López, V., Skaf, M., Manso, J.M., 2020a. Effect of fine recycled concrete aggregate on the mechanical behavior of self-compacting concrete. Construct. Build. Mater. 263, 120671. https://doi.org/10.1016/j.conbuildmat.2020.120671.

Revilla-Cuesta, V., Skaf, M., Chica, J.A., Fuente-Alonso, J.A., Ortega-López, V., 2020b. Thermal deformability of recycled self-compacting concrete under cyclical temperature variations. Mater. Lett. 278, 128417. https://doi.org/10.1016/j.matlet.2020.128417.

Revilla-Cuesta, V., Skaf, M., Faleschini, F., Manso, J.M., Ortega-López, V., 2020c. Self-compacting concrete manufactured with recycled concrete aggregate: an overview. J. Clean. Prod. 262, 121362. https://doi.org/10.1016/j.jclepro.2020.121362.

Roslan, N.H., Ismail, M., Khalid, N.H.A., Muhammad, B., 2020. Properties of concrete containing electric arc furnace steel slag and steel sludge. J. Build. Eng. 28, 101060. https://doi.org/10.1016/j.jobe.2019.101060.

Sainz-Aja, J., Carrascal, I., Polanco, J.A., Thomas, C., Sosa, I., Casado, J., Diego, S., 2019. Self-compacting recycled aggregate concrete using out-of-service railway superstructure wastes. J. Clean. Prod. 230, 945−955. https://doi.org/10.1016/j.jclepro.2019.04.386.

Salehi, H., Mazloom, M., 2019. Opposite effects of ground granulated blast-furnace slag and silica fume on the fracture behavior of self-compacting lightweight concrete. Construct. Build. Mater. 222, 622−632. https://doi.org/10.1016/j.conbuildmat.2019.06.183.

Salesa, Á., Pérez-Benedicto, J.Á., Esteban, L.M., Vicente-Vas, R., Orna-Carmona, M., 2017. Physico-mechanical properties of multi-recycled self-compacting concrete prepared with precast concrete rejects. Construct. Build. Mater. 153, 364−373. https://doi.org/10.1016/j.conbuildmat.2017.07.087.

Santamaría, A., Orbe, A., Losañez, M.M., Skaf, M., Ortega-Lopez, V., González, J.J., 2017. Self-compacting concrete incorporating electric arc-furnace steelmaking slag as aggregate. Mater. Des. 115, 179−193. https://doi.org/10.1016/j.matdes.2016.11.048.

Santamaría, A., González, J.J., Losáñez, M.M., Skaf, M., Ortega-López, V., 2020a. The design of self-compacting structural mortar containing steelmaking slags as aggregate. Cement Concr. Compos. 111, 103627. https://doi.org/10.1016/j.cemconcomp.2020.103627.

Santamaría, A., Ortega-López, V., Skaf, M., Chica, J.A., Manso, J.M., 2020b. The study of properties and behavior of self compacting concrete containing Electric Arc Furnace Slag (EAFS) as aggregate. Ain Shams Eng. J. 11 (1), 231−243. https://doi.org/10.1016/j.asej.2019.10.001.

Santos, S.A., da Silva, P.R., de Brito, J., 2019a. Self-compacting concrete with recycled aggregates − a literature review. J. Build. Eng. 22, 349−371. https://doi.org/10.1016/j.jobe.2019.01.001.

Santos, S.A., da Silva, P.R., de Brito, J., 2019b. Durability evaluation of self-compacting concrete with recycled aggregates from the precast industry. Mag. Concr. Res. 71 (24), 1265−1282. https://doi.org/10.1680/jmacr.18.00225.

Silva, R.V., De Brito, J., Dhir, R.K., 2015. The influence of the use of recycled aggregates on the compressive strength of concrete: a review. Eur. J. Environ. Civ. Eng. 19 (7), 825−849. https://doi.org/10.1080/19648189.2014.974831.

Silva, R.V., de Brito, J., Dhir, R.K., 2018. Fresh-state performance of recycled aggregate concrete: a review. Construct. Build. Mater. 178, 19−31. https://doi.org/10.1016/j.conbuildmat.2018.05.149.

Song, W., Yi, J., Wu, H., He, X., Song, Q., Yin, J., 2019. Effect of carbon fiber on mechanical properties and dimensional stability of concrete incorporated with granulated-blast furnace slag. J. Clean. Prod. 238, 117819. https://doi.org/10.1016/j.jclepro.2019.117819.

Vinay Kumar, B.M., Ananthan, H., Balaji, K.V.A., 2017. Experimental studies on utilization of coarse and fine fractions of recycled concrete aggregates in self compacting concrete mixes. J. Build. Eng. 9, 100−108. https://doi.org/10.1016/j.jobe.2016.11.013.

Wongsa, A., Siriwattanakarn, A., Nuaklong, P., Sata, V., Sukontasukkul, P., Chindaprasirt, P., 2020. Use of recycled aggregates in pressed fly ash geopolymer concrete. Environ. Prog. Sustain. Energy 39 (2), e13327. https://doi.org/10.1002/ep.13327.

Wu, H.L., Jin, F., Bo, Y.L., Du, Y.J., Zheng, J.X., 2018. Leaching and microstructural properties of lead contaminated kaolin stabilized by GGBS-MgO in semidynamic leaching tests. Construct. Build. Mater. 172, 626−634. https://doi.org/10.1016/j.conbuildmat.2018.03.164.

Yang, K.H., Jung, Y.B., Cho, M.S., Tae, S.H., 2015. Effect of supplementary cementitious materials on reduction of CO_2 emissions from concrete. J. Clean. Prod. 103, 774−783. https://doi.org/10.1016/j.jclepro.2014.03.018.

Yang, K.H., Hwang, Y.H., Lee, Y., Mun, J.H., 2019. Feasibility test and evaluation models to develop sustainable insulation concrete using foam and bottom ash aggregates. Construct. Build. Mater. 225, 620−632. https://doi.org/10.1016/j.conbuildmat.2019.07.130.

Zuo, W., She, W., Li, W., Wang, P., Tian, Q., Xu, W., 2019. Effects of fineness and substitution ratio of limestone powder on yield stress of cement suspensions. Mater. Struct. 52 (4), 74. https://doi.org/10.1617/s11527-019-1378-1, 74.